Microwave rectification by a carbon nanotube Schottky diode

Enrique Cobas and Michael S. Fuhrer[a)]
Department of Physics and Center for Nanophysics and Advanced Materials, University of Maryland, College Park, Maryland 20742-4111, USA

(Received 20 February 2008; accepted 5 May 2008; published online 31 July 2008)

Carbon nanotube Schottky diodes have been fabricated in an all-photolithographic process using dissimilar contact metals on high-frequency compatible substrates (quartz and sapphire). Diodes show near-ideal behavior and rectify currents of up to 100 nA and at frequencies of up to 18 GHz. The voltage and frequency dependence is used to estimate the junction capacitance of $\sim 10^{-18}$ F and the intrinsic device cutoff frequency of ~400 GHz. © *2008 American Institute of Physics*.
[DOI: 10.1063/1.2939095]

Due to their high mobility at room temperature,[1,2] semiconducting carbon nanotubes (CNTs) have been proposed for terahertz electronic devices.[3–7] However, the high characteristic impedance (on order the resistance quantum, $R_Q = h/2e^2 = 12.9\ \mathrm{k}\Omega$) of an individual CNT makes measurements of the high-frequency electrical properties of CNT devices especially difficult because of the impedance mismatch to conventional 50 Ω transmission lines. Several solutions to this problem have been explored, including mixing experiments in three-terminal devices to produce low-frequency output,[8,9] impedance matching using a resonant circuit,[10] using multiple CNTs in parallel,[11–13] or calculating high-frequency parameters from low-frequency measurements.[14]

We demonstrate a simple solution to the problem of measuring the high-frequency electrical properties of CNT devices. The Schottky diode formed between a CNT and a metal electrode[14–17] is used as a rectifier to produce a dc in response to a microwave-frequency voltage. We show that this CNT Schottky diode (CNT-SD) can rectify large currents (>100 nA) and operates at frequencies up to 18 GHz. We also find that the intrinsic frequency limit is ~400 GHz and could be much higher if the series resistance of the CNT could be reduced. The Schottky diode can therefore be used as a probe of the local rf power to measure the frequency-dependent conductivity of CNTs and other nanoscale semiconducting devices.

rf-compatible CNT-SD devices were prepared on sapphire and quartz substrates through in the following manner. An array of alumina-supported $Mo_2(acac)_2$ and $Fe(NO_3)_3$ catalyst islands was prepatterned on sapphire and quartz substrates using a polymethylmethacrylate—photoresist double layer photolithography.[18] CNTs (work function of 4.7–5.1 eV) (Refs. 19–21) were grown via chemical vapor deposition at 900 °C in a tube furnace using methane, hydrogen, and ethylene.[22] Contacts and leads for a 360-device array were created in close proximity to the catalyst islands by two steps of standard photolithography. Low-Ohmic contacts were deposited via electron-beam evaporation of 200 Å of platinum (work function of 5.6 eV), followed by 2000 Å of gold and capped with 200 Å of platinum for surface hardness. Schottky contacts were deposited to either side of the central ohmic contact via thermal evaporation of 50 Å of chromium (work function of 4.5 eV) and 2000 Å of gold. Figure 1 shows a completed device. The majority of the devices included no nanotubes or included metallic nanotubes which obscure the transport properties of the semiconducting nanotubes (e.g., device 1 in Fig. 1, which exhibits metallic behavior with $R \sim 50\ \mathrm{k}\Omega$). However, some of the devices included single semiconducting nanotubes (e.g., device 2 in Fig. 1).

All electrical measurements were carried out in a Cascade Microtech Summit 1200 automated probe station using Keithley 2400 SourceMeters under ambient conditions; see supplementary information for more details about the measurement setup.[23] rf measurements were performed using a Hewlett Packard 83620B microwave signal generator, an *X*-band horn antenna, an Ithaco 1211 current amplifier, and a Stanford Research Systems SR 380 lock-in amplifier. The probe station's dc electrical probes doubled as receiver an-

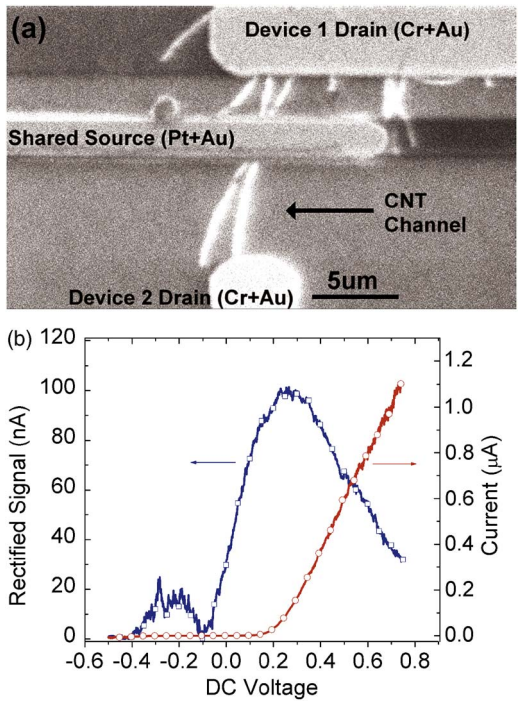

FIG. 1. (Color online) (a) Optical image of the leads comprising devices 1 and 2 and (b) the current-voltage characteristics (red circles) and rectified current signal (blue squares) from device 2 shown, due to a 7 GHz microwave signal at 9 dBm.

a)Electronic mail: mfuhrer@physics.umd.edu.

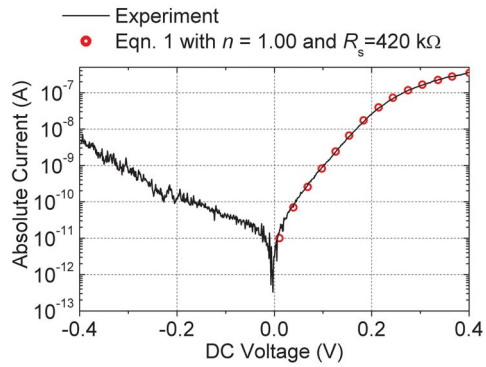

FIG. 2. (Color online) dc current-voltage characteristics of a CNT-SD (black line) and corresponding fit to Eq. (1) (red circles) with $n=1.00$ and $R_s=420$ kΩ. The data shown are from device 2 pictured in Fig. 1.

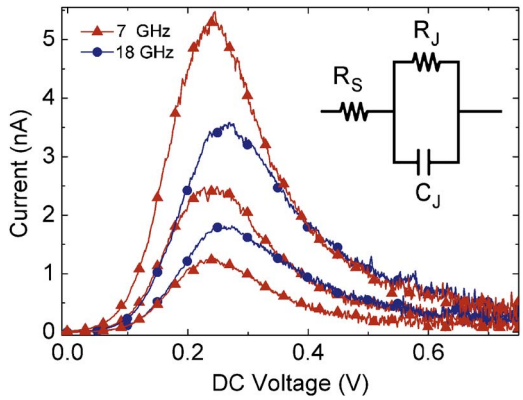

FIG. 3. (Color online) Rectified output signal from a CNT-SD as a function of dc bias under various powers of 7 GHz (red squares) and 18 GHz (blue triangles) microwave excitation. The corresponding microwave intensities are (top to bottom) −14, −17, and −20 dBm for the 7 GHz data and −8 and −11 dBm for the 18 GHz data. The inset shows the model equivalent circuit, ignoring the stray capacitance which is bias independent.

tennae, directing the microwave signal broadcast from the nearby horn antenna into the nanotube device. The microwave signal was amplitude modulated at 1 kHz to enable measurement of the rectified current signal with the lock-in amplifier as a function of microwave frequency, microwave power, and dc bias.

Figure 2 shows the dc current-voltage (I-V) curve for an individual CNT-SD. At low frequency, we model the CNT-SD as a diode in series with a resistor

$$I = I_s[e^{(qV-IR_s)/nkT} - 1], \tag{1}$$

where I_s is the reverse saturation current, R_s is the series resistance, n is the ideality factor, k is Boltzmann's constant, q is the electronic charge, and T is the temperature. A fit to this equation (0–400 mV) gives $n=1.00$ and a series resistance $R_s=420$ kΩ. The diode resistance and series resistance are approximately equal at $V_{dc}\approx 200$ mV, where a knee in the I-V curve is evident.

In general, we found that the response of the device embedded in the measurement setup was strongly dependent on frequency, with the response as a function of frequency showing numerous peaks and valleys. We attribute this to strong dependence of the antenna efficiency on frequency resulting from resonances in our nonideal setup. Thus, using the applied microwave power is a poor indicator of the power reaching the device. Although the complex frequency dependence of our measurement setup makes a simple, direct frequency dependence measurement impossible, a comparison of the bias-voltage dependence of the data at various frequencies within the square-law power regime does lead us to useful conclusions. Figure 3 shows a comparison of rectified current ΔI at frequencies $f=7$ GHz (red) and $f=18$ GHz (blue) at various source powers P within the square-law regime. A systematic difference in the shape of the ΔI-V curve with frequency is evident. This may be understood qualitatively as follows. Consider the two curves corresponding to $f=7$ GHz, $P=-14$ dBm, and $f=18$ GHz $P=-8$ dBm. At high V, when the diode resistance is low, these two curves produce similar response, indicating that the cutoff frequency is much larger than 18 GHz. As V decreases, the diode resistance increases, and the cutoff frequency decreases below 18 GHz so the response becomes frequency dependent, smaller at higher f. We explore this quantitatively below.

We express the power reaching the Schottky junction as

$$P_j = PE_{\text{ant}}E_{\text{dev}}, \tag{2}$$

where P is the emitted power, E_{ant} is the fraction of the emitted power absorbed by the device, and E_{dev} is the fraction of power in the device dissipated at the Schottky junction. Then, the additional current due to the power absorbed in the junction can be expressed as

$$\Delta I = \beta P_j, \tag{3}$$

where the responsivity β is determined solely by the variable junction resistance $R_j(V)$.

Then, following Sorensen and Cowely,[24] we model the device as R_j in parallel with a constant junction capacitance C_j and a constant series resistance R_s, as in Fig. 3 (inset). This leads to expressions for the predicted cutoff frequency f_c in the square-law regime and the frequency-dependent device efficiency $E_{\text{dev}}(f)$

$$f_c = \frac{(1+R_s/R_j)^{1/2}}{2\pi C_j(R_sR_j)^{1/2}}, \tag{4}$$

$$E_{\text{dev}}(f) = \frac{P_j}{P_{\text{dev}}} = \frac{1}{\left(1+\frac{R_s}{R_j}\right)[1+(f/f_c)^2]}. \tag{5}$$

Then, from Eq. (2), the ratio of the currents at two different frequencies is $\Delta I(f_1)/\Delta I(f_2)=[E_{\text{dev}}(f_1)/E_{\text{dev}}(f_2)]\times[E_{\text{dev}}(f_1)/E_{\text{dev}}(f_2)]=\text{const}\times[E_{\text{dev}}(f_1)/E_{\text{dev}}(f_2)]$. The signal strength was verified to be proportional to the microwave power, indicating that the device was operating in the square-law regime. The ratio of the device efficiencies at frequencies f_1 and f_2 approaches the values $E_{\text{dev}}(f_1)/E_{\text{dev}}(f_2)=1.00$ for $(f_1,f_2\ll f_c)$ and $E_{\text{dev}}(f_1)/E_{\text{dev}}(f_2)=(f_2/f_1)^2$ (which is a factor of 6.61 for the two frequencies used here) for $(f_1,f_2\gg f_c)$. Since R_j and hence f_c are strong functions of bias voltage, in general, there will be a transition from $f_1,f_2\gg f_c$ to $f_1,f_2\ll f_c$, and the ratio $\Delta I(f_1)/\Delta I(f_2)$ will be bias-voltage dependent.

Figure 4 shows a comparison of the efficiency ratio for various trial junction capacitances C_J and the ratio of the experimentally measured 7 and 18 GHz signals, ΔI (7 GHz)/ΔI (18 GHz), which as anticipated above, is volt-

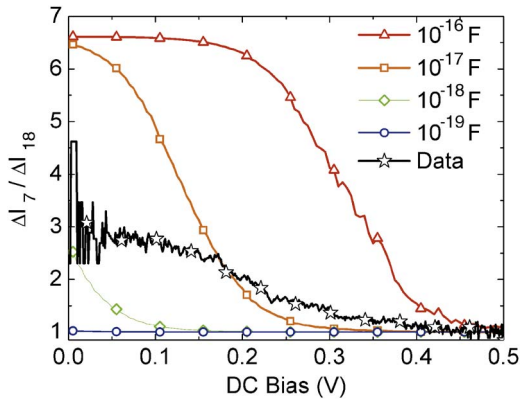

FIG. 4. (Color online) Rectified current ratio at 7 GHz vs 18 GHz as a function of dc bias. Solid lines are calculated from the measured junction resistance data $R_j(V)$ and the model equivalent circuit in Fig. 3 for junction capacitances $C_j = 10^{-19}$ F (blue circles), 10^{-18} F (green rhombi), 10^{-17} F (orange squares), and 10^{-16} F (red triangles). The experimentally observed ratio (scaled to 1.0 at high bias) is shown as black stars.

age dependent. The experimental ratio varies more gradually with voltage than the theoretical curves. This is likely due to the fact that R_s and C_j are distributed elements along the length of the CNT; as R_j becomes small (large V) and the resistance is dominated by the series resistance of the CNT, the capacitive coupling of portions of the CNT more distant from the junction becomes relatively more important, and the effective C_j increases. However, comparing the large V and small V limits we can conclude that the junction capacitance of the device is in the 10^{-18} F range, in accordance with previous estimates.[25–27] This value allows us to estimate the intrinsic nanotube diode cutoff frequency $f_c = 1/2\pi RC_j = 1/2\pi(420\ \mathrm{k}\Omega)(10^{-18}\ \mathrm{F}) \approx 400$ GHz.

We have demonstrated fabrication of CNT-SDs via straightforward CNT synthesis and lithography techniques. The devices produced exhibit excellent Schottky diode characteristics with ideality factors n close to unity, in series with a high channel resistance and exhibit good rectification performance beyond 7 GHz. We have also demonstrated a simple technique for observation of microwave rectification in nanoscale semiconductor devices. The intrinsic cutoff frequency set by the junction capacitance and series resistance of CNT-SDs is in the order of 400 GHz and could be pushed into the terahertz if the series resistance could be lowered, e.g., through shortening or doping the CNT. Measurements on an additional CNT-SD (see supplementary information)[23] indicate that the series resistance can be reduced by shortening the CNT.

We acknowledge support from the Army Research Laboratory MICRA program, the shared equipment facilities of the UMD-MRSEC, and thank Dr. Steven Anlage for useful discussions and use of his microwave equipment.

[1] T. Durkop, S. Getty, E. Cobas, and M. S. Fuhrer, Nano Lett. **4**, 35 (2004).
[2] V. Perebeinos, J. Tersoff, and P. Avouris, Nano Lett. **6**, 205 (2005).
[3] P. J. Burke, Solid-State Electron. **48**, 1981 (2004).
[4] S. H. Jing Guo, A. Javey, G. Bosman, and M. Lundstrom, IEEE Trans. Nanotechnol. **4**, 715 (2005).
[5] K. Alam and R. K. Lake, J. Appl. Phys. **100**, 024317 (2006).
[6] L. C. Castro, D. L. Pulfrey, and D. L. John, Solid State Phenom. **121-123**, 693 (2007).
[7] D. Dragoman and M. Dragoman, Physica E (Amsterdam) **25**, 492 (2005).
[8] A. A. Pesetski, J. E. Baumgardner, E. Folk, J. Przybysz, J. Adam, and H. Zhang, Appl. Phys. Lett. **88**, 113103 (2006).
[9] S. Rosenblatt, H. Lin, V. Sazonova, S. Tiwari, and P. McEuen, Appl. Phys. Lett. **87**, 153111 (2005).
[10] S. Li, Z. Yu, S.-F. Yen, W. C. Tang, and P. J. Burke, Nano Lett. **4**, 753 (2004).
[11] X. Huo, M. Zhang, P. C. H. Chan, Q. Liang, and Z. K. Tang, Tech. Dig. - Int. Electron Devices Meet. **2004**, 691.
[12] J. M. Bethoux, H. Happy, G. Dambrine, V. Derycke, M. Goffman, and J. P. Bourgoin, IEEE Electron Device Lett. **27**, 681 (2006).
[13] T.-I. Jeon, K.-J. Kim, C. Kang, I. H. Maeng, J.-H. Son, K. H. Son, K. H. An, J. Y. Lee, and Y. H. Lee, J. Appl. Phys. **95**, 5736 (2004).
[14] H. Manohara, E. Wong, E. Schlect, B. D. Hunt, and P. H. Siegel, Nano Lett. **5**, 1469 (2005).
[15] S. Heinze, J. Tersoff, R. Martel, V. Derycke, J. Appenzeller, and Ph. Avouris, Phys. Rev. Lett. **89**, 106801 (2002).
[16] F. Leonard and J. Tersoff, Phys. Rev. Lett. **84**, 4693 (2000).
[17] W. Zhu and E. Kaxiras, Appl. Phys. Lett. **89**, 243107 (2006).
[18] J. Kong, H. Soh, A. Cassell, C. Quate, and H. Dai, Nature (London) **395**, 878 (1998).
[19] S. Suzuki, Y. Watanabe, Y. Homma, S. Fukuba, S. Heun, and A. Locatelli, Appl. Phys. Lett. **85**, 127 (2004).
[20] S. Suzuki, C. Bower, Y. Watanabe, and O. Zhou, Appl. Phys. Lett. **76**, 4007 (2000).
[21] K. Okazaki, Y. Nakato, and K. Murakoshi, Phys. Rev. B **68**, 035434 (2003).
[22] W. Kim, H. C. Choi, M. Shim, Y. Li, D. Wang, and H. Dai, Nano Lett. **2**, 703 (2002).
[23] See EPAPS Document No. E-APPLAB-92-006823 for a description of the measurement setup and data on an additional device. For more information on EPAPS, see http://www.aip.org/pubservs/epaps.html.
[24] H. O. Sorensen and A. M. Cowley, IEEE Trans. Microwave Theory Tech. **MTT-14**, 588 (1966).
[25] P. Jarillo-Herrero, S. Sapmaz, C. Dekker, L. P. Kowenhoven, and H. S. H. J. van der Zant, Nature (London) **429**, 389 (2004).
[26] H. W. C. Postma, T. Teepen, Z. Yao, M. Grifoni, and C. Dekker, Science **293**, 76 (2001).
[27] R. Tarkiainen, M. Ahlskog, J. Penttila, L. Roschier, P. Hakonen, M. Paalanen, and E. Sonin, Phys. Rev. B **64**, 195412 (2001).